

# Precise Water Isotope Analysis in the Natural Concentration Range Using Off-Axis Integrated Cavity Output Spectroscopy (OA-ICOS)

Amir Asgary<sup>a,b</sup>, Babak Jaleh<sup>a,\*</sup>

<sup>a</sup>Faculty of Science, Bu-Ali Sina University, Hamedan, Iran

<sup>b</sup>Institute of Molecular Sciences and Engineering, Arak University, Arak, Iran

Corresponding author email: [jaleh@basu.ac.ir](mailto:jaleh@basu.ac.ir)

Received: Dec. 18, 2024, Revised: June 20, 2025, Accepted: July 13, 2025, Available Online: July 15, 2025

DOI: will be added soon

**ABSTRACT**— A compact sensor utilizing off-axis integrated cavity output spectroscopy at a wavelength of 1.389  $\mu\text{m}$  was developed to measure the  $\delta^{18}\text{O}$  and  $\delta^2\text{H}$  isotopic ratios in liquid water samples within the natural concentration range. Allan variance analysis indicated an optimal averaging time of approximately 21 s. The stability and long-term reproducibility of the laser system were assessed using 1-second averaging over 75 min. The minimum detectable absorption (MDA) was determined to be approximately  $8.4 \times 10^{-4} \text{ Hz}^{-1/2}$  with a 17 s averaging time. To assess accuracy and reproducibility, the setup was tested within the natural concentration range ( $\delta^2\text{H}$ : -400 to 0‰ and  $\delta^{18}\text{O}$ : -54 to 0‰) using five standard samples, achieving an average accuracy and reproducibility of better than 2.5‰ for  $\delta^2\text{H}$  and 0.5‰ for  $\delta^{18}\text{O}$ .

**KEYWORDS:** Water Isotopes, Natural concentration, Laser Spectroscopy, Allan deviation, Sensitivity, Accuracy, Averaging.

## I. INTRODUCTION

The transitions of water between its vapor, liquid, and ice phases are fundamental physicochemical processes that lead to variations in the abundances of oxygen and hydrogen isotopes in natural waters. These changes occur during evaporation and precipitation (hydrological processes) as well as boiling and freezing in the atmosphere, on the surface, and in the upper layers of the Earth's crust. Understanding these isotopic,

particularly between liquid water and water vapor, is crucial for tracing natural water sources [1].

The first measurements of the isotopic abundance of water were conducted by H.C. Urey at the University of Chicago in 1932. A mass spectrometer with two inlets and two collectors was used for these isotopic measurements. The results of these studies indicated that freshwater samples gradually deplete heavier isotopes, while the residual evaporation of surface waters (hydrological processes), such as those from Africa's lakes, becomes enriched in oxygen and hydrogen isotopes, resulting in heavier water [2]. These measurements were conducted to gain a better understanding of the processes related to the water cycle by utilizing isotopic abundance in various regions on the Earth's surface, such as lakes and oceans. Over time, methods for measuring the isotopic abundance of water in different areas of the Earth's surface and atmosphere have improved, enhancing measurement accuracy [3]-[5].

To date, several methods have been developed for identifying various substances, including  $\text{H}_2\text{O}$ , and determining their isotopic ratios. The most well-known methods are mass spectrometry, Fourier-transform infrared spectroscopy, and laser spectroscopy [6]. Laser spectroscopy is now considered an attractive method for identifying and measuring various

elements and isotopes across a wide range of fields, including meteorology, geology, medicine, ecosystems, and astrobiology. It is a highly practical method for analyzing elements, as it does not require sample preparation and is suitable for analyzing samples containing isotopes with similar masses [7].

Tunable Diode Laser Absorption Spectroscopy (TDLAS) is a laser spectroscopy technique that employs a tunable diode laser with a very narrow frequency bandwidth to emit light at specific wavelengths, which can be adjusted to match the absorption features of target gas molecules. As the laser light passes through a sample, the amount of light absorbed by the gas is measured, allowing for precise determination of gas concentrations. These measurements can be classified into two types: direct measurements and indirect methods. Indirect methods include the use of Fabry-Perot cavities and multi-pass cells, which enhance sensitivity by allowing multiple passes of the laser light through the sample. The sensitivity of the direct method is relatively low due to the minimal interaction of the laser beam with the material in the selected laser frequency region [8].

In the field of gas detection in the infrared region, Fabry-Perot cavities are commonly used tools that increase the effective absorption path length, thereby improving detection sensitivity. Methods that utilize Fabry-Perot cavities are known as cavity-enhanced absorption spectroscopy (CEAS) and can be classified into two main types: cavity ring-down spectroscopy (CRDS) and off-axis integrated cavity output spectroscopy (OA-ICOS). Each of these methods has undergone significant improvements over the past two decades since their initial reports by Keefe in 1988 and Paul in 2001 [9], [10].

The Fabry-Perot cavities used in cavity absorption spectroscopy face challenges related to the overlap of optical designs on mirrors, the generation of fringes, and consequently, the reduction of the signal-to-noise ratio and system sensitivity. In this study, the OA-ICOS method was employed to measure the isotopic composition of water with high precision,

enabling a detailed analysis of the water cycle and its variations across different regions. This method offers rapid analysis and ease of use, making it an attractive alternative for many applications [11]-[13].

## II. THEORY

When light interacts with a wavelength corresponding to the absorption characteristics of a molecule, absorption occurs, resulting in a change in the intensity of the output light at that wavelength. By measuring the intensity of the output light and comparing it to the initial light intensity, along with performing calculations, one can determine the concentration of the substances present.

Based on the Beer-Lambert law, the absorption  $A(\nu)$  is related to the intensities of the transmitted light  $I(\nu)$  and the incident light  $I_0(\nu)$  from the sample as follows [14]:

$$A(\nu) = \ln \left[ \frac{I_0(\nu)}{I(\nu)} \right] = C\sigma(\nu)L \quad (1)$$

which  $C$  represents the molecular concentration (molecule/cm<sup>3</sup>),  $\sigma(\nu)$  is the absorption cross-section (cm<sup>2</sup>/molecule), and  $L$  is the optical path length through the absorbing sample (cm).

By integrating the area under the absorption peak  $A(\nu)$  in the frequency range around the center frequency, due to peak broadening (natural, Doppler, and collisional broadening) corresponding to different isotopes of water, we will be able to determine the isotopic ratios  $\delta^2H$  and  $\delta^{18}O$  using the calibration curve obtained from known standards.

To enhance measurement sensitivity, a multi-pass Fabry-Perot cavity is employed. The frequency modes of the cavity are known as Fabry-Perot modes. A Fabry-Perot interferometer consists of two highly reflective surfaces that can produce modes with a very narrow bandwidth  $\Delta\nu_{1/2}$ , commonly referred to as high finesse, and a free spectral range  $\delta\nu$ . The free spectral range (the frequency

difference between Fabry-Perot modes) and the full width at half maximum (FWHM) of each mode are given by the following equations:

$$\delta\nu = \frac{c}{2d\sqrt{n^2 - \sin^2 \alpha}} \quad (2)$$

$$\Delta\nu_{1/2} = \frac{c}{2nd} \cdot \frac{1-R}{\pi\sqrt{R}} \quad (3)$$

where  $c$  is the speed of light in cm/s,  $d$  is the distance between the two reflective surfaces (high-reflectivity mirrors)(cm),  $n$  is the refractive index,  $\alpha$  is the angle of light incidence into the cavity relative to the optical axis (radian), and  $R$  is the reflectivity of the mirrors used. As can be observed, increasing the reflectivity of the mirrors results in a decrease in the frequency width of the amplified modes. In this context, the finesse parameter for on-axis configuration ( $\alpha = 0$ ) is defined as follows [15]:

$$F = \frac{\delta\nu}{\Delta\nu_{1/2}} = \frac{\pi\sqrt{R}}{1-R} \quad (4)$$

in the on-axis configuration of the CRDS (Cavity Ring-Down Spectroscopy) method, where the laser beam is aligned along the optical axis of the cylindrical cavity, the reduction of the frequency width  $\delta\nu$  is constrained by the cavity length. In contrast, in the off-axis configuration, adjusting the angle  $\alpha$  away from zero leads to the formation of a dense mode spectrum, characterized by very small frequency differences between the modes within the cavity. This configuration allows for precise and random coupling of the laser to the cavity modes.

The natural range of isotopic ratios for water is  $\delta^2H = -400$  to  $0\%$  and  $\delta^{18}O = -54$  to  $0\%$ . Conventionally, isotopic ratios are expressed using  $\delta$  notation, with the unit being per mil ( $\%$ ). The relative deviation of the isotopic ratio of a rare isotope compared to that of an enriched isotope in a sample (for  $\delta^2H$ , the enriched isotope is  $H_2^{16}O$  and the rare isotope is

$H_2^{18}O$ ) is measured relative to a standard material,  $\delta$ . The relationship is as follows:

$$\delta^2H = \left( \left( \frac{R_{sample}}{R_{reference}} \right) - 1 \right) \times 1000 \quad (5)$$

$$\delta^{18}O = \left( \left( \frac{R_{sample}}{R_{reference}} \right) - 1 \right) \times 1000 \quad (6)$$

where  $R_{sample}/R_{reference}$  is the ratio of the concentration of the rare isotope to the enriched one, and its unit is ppm (parts per million).  $R_{reference}$  indicates the isotopic composition of a known standard, while  $R_{sample}$  represents the isotopic composition of the sample being analyzed. Since the variations in the  $\delta$  value is small, it is common to express measurements in per mil ( $\%$ ) unit to specify the isotopic ratio. The reference value corresponds to the natural range and is referred to as VSMOW (Vienna Standard Mean Ocean Water). The isotopic ratios  $R(^2H/{}^1H)$  and  $R(^{18}O/{}^{16}O)$  related to this reference are 155.76 ppm and 2005.25 ppm, respectively.

### III. EXPERIMENTAL SETUP

The schematic structure of the system is illustrated in Fig. 1. To excite the vibrational modes of water molecules, a Distributed Feedback (DFB) diode laser emitting in the near-infrared region with a wavelength of approximately  $1.389 \mu m$  and a bandwidth of about 2 MHz is utilized. The laser beam enters the space between two highly reflective mirrors (with reflectivity) around 99.98%) in an off-axis configuration relative to the main axis of the cavity. The cavity is constructed from stainless steel, with optical holders containing highly reflective mirrors positioned on both sides.

By applying a sawtooth waveform to the DFB laser driver (which control temperature and current of laser chip) and appropriately adjusting the laser temperature, the desired frequency range corresponding to the three absorption peaks of the isotopes  $H_2^{16}O$ ,

$^1\text{H}^2\text{H}^{16}\text{O}$ , and  $\text{H}_2^{18}\text{O}$  is investigated. The transmitted signal from the cavity is affected by the presence of water vapor from the injected sample in the space between the mirrors, where it interacts with the laser beam. This occurs after the system has been evacuated to approximately 20 mbar using a vacuum pump. The interaction leads to the absorption of specific wavelengths, resulting in distinct absorption peaks for the isotopes  $\text{H}_2^{18}\text{O}$ ,  $\text{H}_2^{16}\text{O}$ , and  $^1\text{H}^2\text{H}^{16}\text{O}$ .

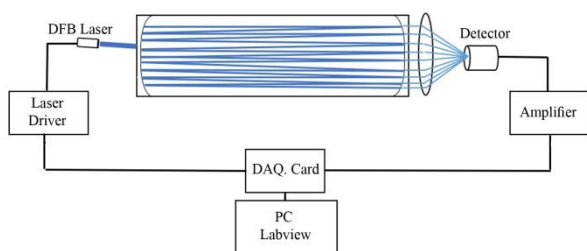


Fig. 1. Experimental setup of water isotope analyzer.

Figure 2 displays the averaged transmission spectrum of the natural concentration water vapor sample, along with its polynomial fit and the identified absorption peaks.

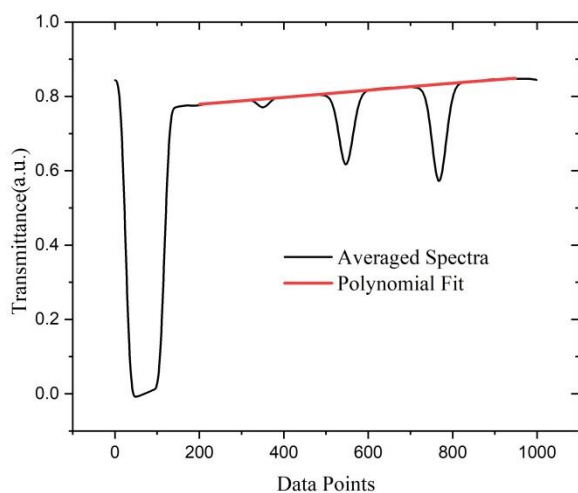


Fig. 2. The averaged transmission spectrum of the natural concentration water vapor sample along with its polynomial fit.

The ground state energy, line strength, and changes in the isotopic ratios  $\delta^2\text{H}$  and  $\delta^{18}\text{O}$  as a function of temperature variations are summarized in Table 1.

The spectrum corresponding to a sawtooth scan of the laser is presented in Fig. 2. Located behind the second mirror is a convex lens with a focal length of approximately 3 cm. This lens

plays a crucial role in focusing the light transmitted from behind the second mirror. As the laser beam reflects off the second mirror, a small portion of the beam passes through and reaches the lens. The convex lens then focuses this transmitted light onto an InGaAs detector, thereby enhancing the intensity and clarity of the signal that is ultimately detected. The signals received from the detector are amplified and processed in real-time on a computer using a high-speed data acquisition card (approximately 600 kS/s) with LabVIEW software.

By removing the sawtooth background from the transmission spectrum, the absorption spectrum is obtained, as shown in Fig. 3. After applying various filters, including low-pass and high-pass filters, and fitting the final data with a Voigt profile, we can determine the area under the curve for the three isotopes under investigation. This allows us to report the area ratios of the peaks  $\text{H}_2^{18}\text{O}/\text{H}_2^{16}\text{O}$  and  $^1\text{H}^2\text{H}^{16}\text{O}/\text{H}_2^{16}\text{O}$ .

Subsequently, by measuring the area ratios under the isotopic peaks corresponding to known concentration standards and plotting a calibration curve, we can determine the final isotopic ratio for each sample per mil (%) as the  $\delta$  value. This value is calculated using the established calibration curve.

Table 1. List of the parameters for the absorption lines used in this study

Absorption Peaks Specifications	$\text{H}_2^{18}\text{O}$	$\text{H}_2^{16}\text{O}$	$^1\text{H}^2\text{H}^{16}\text{O}$
Frequency( $\text{cm}^{-1}$ )	7199.96	7200.13	7200.30
Line Strength ( $\times 10^{-24}$ cm. molecule $^{-1}$ )	4.469	3.07	0.189
Ground State Energy( $\text{cm}^{-1}$ )	505.72	315.77	615.96
Temperature Coefficient related to $\text{H}_2^{16}\text{O}$ Reference Peak at 296 K	+3.12	-	-4.9

## IV. RESULTS

According to Fig. 3, the minimum detectable absorption of the system, taking into account the data acquisition rate and the standard deviation of the residuals from the Voigt fit, is

determined for the averaged absorption spectrum as follows:

$$\text{MDA} = \left( \frac{\Delta p}{p} \right) \times \left( \frac{1}{\sqrt{BW}} \right) \quad (7)$$

where  $BW = b\omega/n$  denotes the ratio of data acquisition frequency ( $b\omega$ ) to the number of laser scans ( $n$ ). The term  $(\Delta p/p)$  denotes the ratio of the standard deviation of the residuals from the Voigt function fit ( $\Delta p$ ) to the maximum absorption ( $p$ ) shown in Fig. 3, measured over a specified data acquisition duration [16]. These fluctuations arise from the overlap of the laser beam on the mirrors and contribute to a reduction in the signal-to-noise ratio. With a data acquisition speed of approximately 600 kHz and duration of 17s, the minimum detectable absorption, based on the results extracted from Fig. 3, is approximately  $8.4 \times 10^{-4} \text{ Hz}^{-1/2}$ .

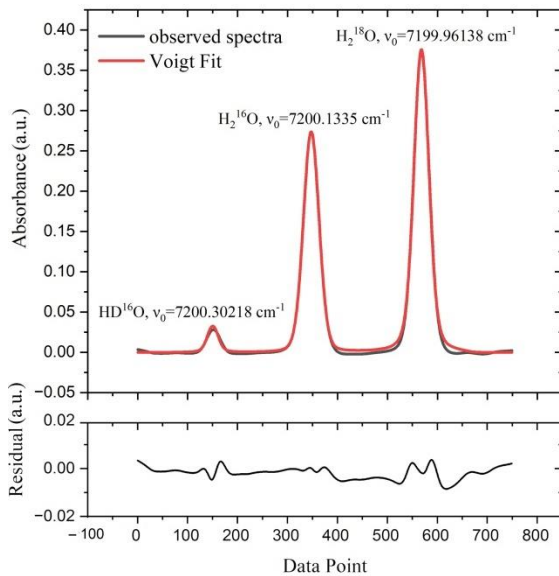


Fig. 3. Voigt Fit and residuals of absorption isotope peak of water.

To assess the repeatability and stability of the current system, data on the isotopic ratios  $\delta^2H$  and  $\delta^{18}O$  were recorded in situ with a data acquisition and averaging time of one second over 75 min. The results are displayed in Fig. 4. Additionally, to evaluate the system's stability over varying data acquisition durations and to determine the optimal averaging time, the Allan variance curve is plotted in Fig. 5. As shown,

optimal stability of the laser system is achieved with approximately 21s of data acquisition [17].

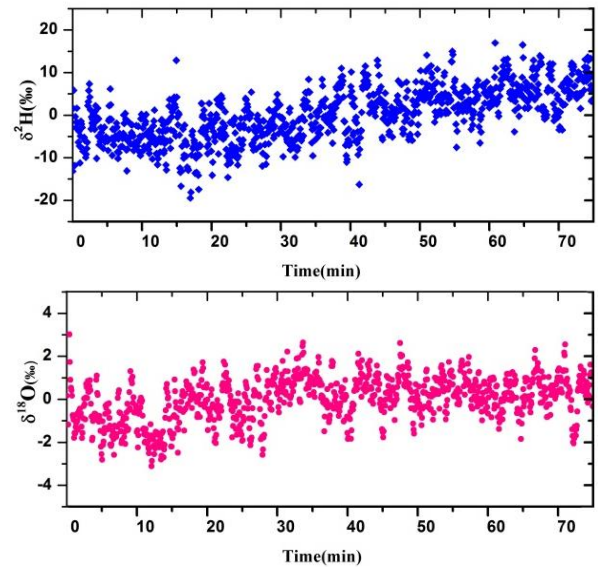


Fig. 4. Measurement of  $\delta^2H$  and  $\delta^{18}O$  with one second of data acquisition to assess the long-term stability of the results.

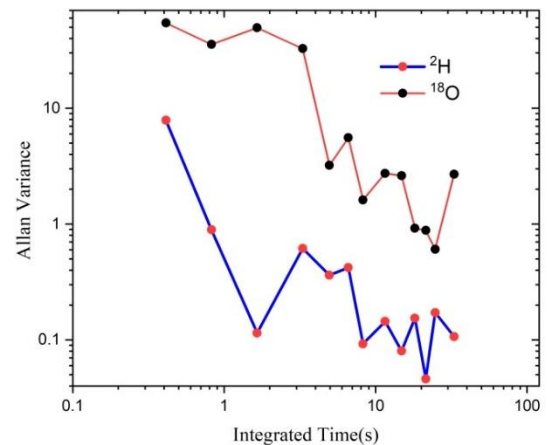


Fig. 5. Allan variance curve related to different data acquisition times.

Figure 6 illustrates the short-term repeatability for 22 injections of natural water samples at a specified concentration. Each measurement lasts approximately 100 seconds, resulting in a total measurement time of 33 min. Data points exceeding three times the average difference was excluded from the analysis. The standard deviations for the data presented in Fig. 6 are 0.97‰ for  $\delta^2H$  and 0.21‰ for  $\delta^{18}O$  [17].

Finally, Fig. 7 shows the measurement sensitivity for reading specific samples, using standard samples with the specifications listed in Table 2.

The findings indicate that the system achieved an average accuracy and reproducibility better than 2.5‰ for  $\delta^2H$  and 0.5‰ for  $\delta^{18}O$ . The high precision of  $\delta^{18}O$  and  $\delta^2H$  measurements suggest strong consistency and reliability. These results confirm the robustness of the system, making it highly suitable for applications requiring precise isotopic analysis, such as paleoclimate studies and hydrological modeling.

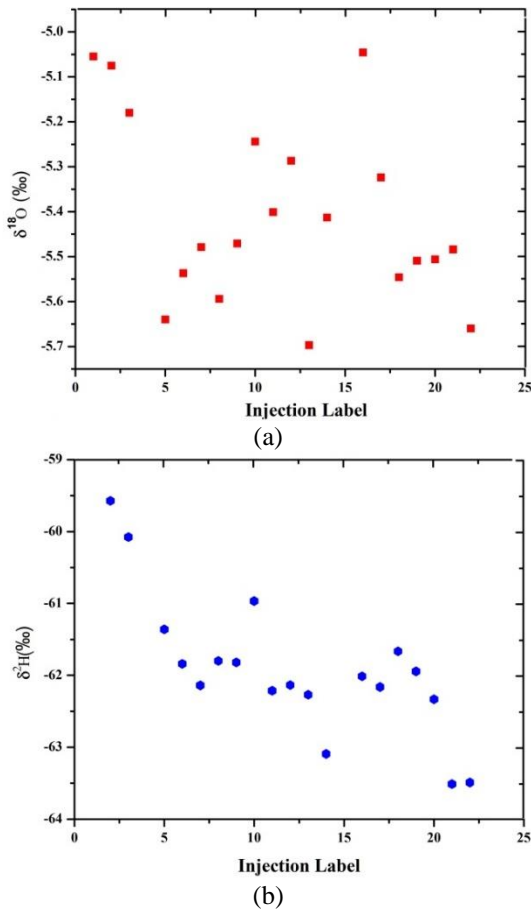


Fig. 6. Results related to the repeatability of the present laser system, 22 injections of identical samples a)  $\delta^2H$  and b)  $\delta^{18}O$ .

Table 2. Standard samples with specific concentrations (standards 2 to 4 were read in a two-point manner)

Standard	$\delta^2H$ (‰)	$\delta^{18}O$ (‰)
1	-262.64	-31.55
2	-185.41	-21.18
3	-113.57	-13.7
4	-53.42	-7.26
5	4.88	1.19

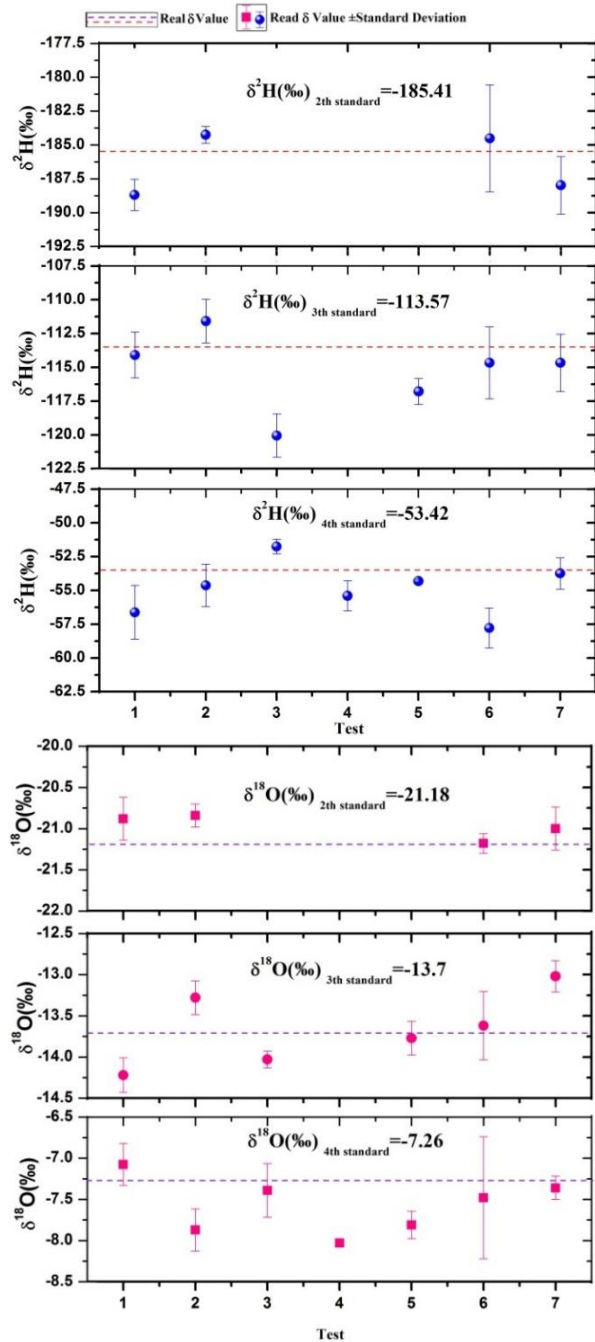


Fig. 7. The  $\delta^2H$  and  $\delta^{18}O$  results are related to the accuracy of the present laser system readings, which range from 4 to 7 across three different samples. The dashed line indicates the actual concentration of the samples, and the error bars on each result represent the measurement precision after five repetitions. The measurement precision is expressed as the  $\pm$  standard deviation of the results.

### V. CONCLUSION

This study demonstrated that the isotopic sensor enables the simultaneous measurement of the isotopic ratios  $\delta^2H$  and  $\delta^{18}O$  in water within the natural range, achieving appropriate accuracy and precision for various scientific

applications. The system's short-term and long-term repeatability were assessed, and its accuracy was validated using standard samples with known values, achieving precisions better than 2.5‰ for  $\delta^2H$  and 0.5‰ for  $\delta^{18}O$ .

These findings confirm that the laser system is a viable method for measuring isotopic ratios in liquid water within its natural concentration range. The system offers several key advantages, including rapid and direct analysis of liquid samples, significantly lower construction and acquisition costs, minimal operator expertise requirements, and no need for sample preparation. The system's stability, repeatability, and accurate readings across various samples within the natural range establish its reliability for research applications in hydrology, meteorology, oceanography, and related fields. Furthermore, with optimizations such as enhancing the signal-to-noise ratio, extending the optical path length, and minimizing electrical and optical noise, the isotopic sensor has the potential to achieve even greater accuracy and precision.

## REFERENCES

- [1] J. Horita and D.J. Wesolowski, "Liquid-vapor fractionation of oxygen and hydrogen isotopes of water from the freezing to the critical temperature," *Geochim. Cosmochim. Acta*, Vol. 58, pp. 3425-3437, 1994.
- [2] J.R. Gat, "Oxygen and hydrogen isotopes in the hydrologic cycle," *Ann. Rev. Earth Planet. Sci.*, Vol. 24, pp. 225-262, 1996.
- [3] J. Galewsky, H.C. Steen-Larsen, R.D. Field, J. Worden, C. Risi, and M. Schneider, "Stable isotopes in atmospheric water vapor and applications to the hydrologic cycle," *Rev. Geophys.*, Vol. 54, pp. 809-865, 2016.
- [4] E. Kerstel and L. Gianfrani, "Advances in laser-based isotope ratio measurements: selected applications," *Appl. Phys. B*, Vol. 92, pp. 439-449, 2008.
- [5] J. Gat, *Isotope Hydrology: A study of the water cycle*, Vol. 6, World Scientific, 2010.
- [6] E. Kerstel, "Isotope ratio infrared spectrometry," in *Handbook of Stable Isotope Analytical Techniques*, Elsevier, pp. 759-787, 2004.
- [7] W. Demtröder, "Applications of Laser Spectroscopy," in *Laser Spectroscopy 2: Experimental Techniques*, 2<sup>nd</sup> Ed., Springer, pp. 589-650, 2015.
- [8] M. Lackner, "Tunable diode laser absorption spectroscopy (TDLAS) in the process industries—a review," *Rev. Chem. Eng.*, Vol. 23, pp. 65-147, 2007.
- [9] A. O'Keefe and D.A.G. Deacon, "Cavity ring-down optical spectrometer for absorption measurements using pulsed laser sources," *Rev. Sci. Instrum.*, Vol. 59, pp. 2544-2551, 1988.
- [10] J.B. Paul, L. Lapson, and J.G. Anderson, "Ultrasensitive absorption spectroscopy with a high-finesse optical cavity and off-axis alignment," *Appl. Opt.*, Vol. 40, pp. 4904-4910, 2001.
- [11] K. Zheng, C. Zheng, H. Zhang, G. Guan, Y. Zhang, Y. Wang, and F.K. Tittel, "A novel gas sensing scheme using near-infrared multi-input multi-output off-axis integrated cavity output spectroscopy (MIMO-OA-ICOS)," *Spectrochim. Acta A*, Vol. 256, p. 119745, 2021.
- [12] E.S. Berman, N.E. Levin, A. Landais, S. Li, and T. Owano, "Measurement of  $\delta^{18}O$ ,  $\delta^{17}O$ , and  $^{17}O$ -excess in water by off-axis integrated cavity output spectroscopy and isotope ratio mass spectrometry," *Anal. Chem.*, Vol. 85, pp. 10392-10398, 2013.
- [13] L. Shao, J. Mei, J. Chen, T. Tan, G. Wang, K. Liu, and X. Gao, "Recent advances and applications of off-axis integrated cavity output spectroscopy," *Microw. Opt. Technol. Lett.*, Vol. 65, pp. 1489-1505, 2023.
- [14] T. Wu, W. Chen, E. Fertein, P. Masselin, X. Gao, W. Zhang, Y. Wang, and J. Koeth, "Measurement of the D/H,  $^{18}O/^{16}O$ , and  $^{17}O/^{16}O$  isotope ratios in water by laser absorption spectroscopy at 2.73  $\mu m$ ," *Sensors*, Vol. 14, pp. 9027-9045, 2014.
- [15] W. Demtröder, "Experimental Techniques in Atomic and Molecular Physics," in *Atoms, Molecules and Photons: An Introduction to Atomic, Molecular and Quantum Physics*, pp. 393-452, 2018.
- [16] E.J. Moyer, D.S. Sayres, G.S. Engel, J.M. St. Clair, F.N. Keutsch, N.T. Allen, J.H. Kroll, and J.G. Anderson, "Design considerations in high-sensitivity off-axis integrated cavity output

spectroscopy,” *Appl. Phys. B*, Vol. 92, pp. 467-474, 2008.

- [17] X. Cui, W. Chen, MW. Sigrist, E. Ferrein, P. Flament, K. De Bondt, and N. Mattielli, “Analysis of the stable isotope ratios ( $^{18}\text{O}/^{16}\text{O}$ ,  $^{17}\text{O}/^{16}\text{O}$ , and D/H) in glacier water by laser spectrometry,” *Anal. Chem.*, Vol. 92, pp. 4512-4517, 2020.



**Amir Asgary** is a PhD student specializing in Laser Optics at Bu-Ali Sina University, Under the supervision of Professor Babak Jaleh. In recent years, he has been actively engaged in the field of laser spectroscopy.



**Babak Jaleh** received his Ph.D. in 2004 from Amirkabir University of Technology, Tehran, Iran. Presently, he is a Professor of Physics Optic and Laser) at Bu Ali Sina University, Hamedan, Iran. He has published over 153 research articles (citations>5800). He is also included in Stanford University’s “Ranking of the World Scientists: World’s Top 2% Scientists” from 2019 to 2023.

Professor Jaleh is the head of the Central Laboratory of Bu Ali Sina University. He is the head of the Laser and Nanocomposite Lab at the faculty of science.